

Spectroscopic studies of neutron rich nuclei above ^{132}Sn

Seminari di gruppo IV – Giovedì 10/10

D. Bianco
ENS di Cachan e IRSN

Outline

1) The general framework

- Introduction - the Nuclear Shell Model
- Solving the associated Schrödinger equation - currently adopted algorithms
- A new method and its endowed sampling procedure

2) Microscopic approaches for studying collectivity

- Collectivity and single particle motion
- Mixed-symmetry states
- Collectivity below and above ^{132}Sn
- Conclusions

Nuclear Shell Model - 1

$$H\Psi^\alpha = (H_0 + V)\Psi^\alpha = E\Psi^\alpha$$

- Model Space

$$\left\{ \Phi_i \right\}_{i=1}^d H_0 \Phi_j = E_0^j \Phi_j$$

- Effective Interaction

$$H_{eff} = PH_0P + PV\Omega$$

Wave operator Ω : $\Psi^\alpha = \Omega \Psi_0^\alpha = \Omega P\Psi^\alpha$

- Direct Methods (“Andreozzi-Lee-Suzuki”, *F. Andreozzi, Phys. Rev. C, 1996*)
- Perturbative methods(Brillouin e Wigner ; Rayleigh e Schrödinger)

Nuclear Shell Model - 2

Infinite Space, A nucleons $\mathbf{H}\psi_{\alpha} = E_{\alpha}\psi_{\alpha}$



Model Space, v nucleons

$$\mathbf{H}_{\text{eff}}\phi_{\alpha} = E_{\alpha}\phi_{\alpha}$$

Problem : even the effective Hamiltonian can be very large

^{116}Sn , $N \sim 10^7$

^{130}Xe , $N \sim 10^9$

^{128}Xe , $N \sim 10^{10}$

Hamiltonian matrix diagonalization - 1

- The solution of the eigenvalue problem requires the diagonalization of the many-body Hamiltonian H in a space of very large dimensions
- Standard diagonalization methods are really time-consuming: their complexity is proportional to N^3
- In most cases, only a few (very often one) eigenstates of a given J and T are needed.
- The non zero matrix elements of H grow only linearly with N
- Adaptive diagonalization algorithms which efficiently identify the relevant pieces of H are more suitable

Hamiltonian matrix diagonalization - 2

Two very successful approaches :

- **Lanczos** (Arnoldi) algorithm for finding the extremal eigenvalues of a symmetric (Hermitean) matrix (see, for instance, E. Caurier et al. Rev. Mod. Phys. 77, 427 (2005) for a review);
- **Stochastic method** : Shell Model Monte-Carlo (**SMMC**) S. E. Koonin, D.J. Dean, and K.Langanke, Phys. Repts. 278, 2 (1997).

Hamiltonian matrix diagonalization - 3

Another possibility: truncation methods

- Quantum Monte-Carlo Diagonalization (**QMCD**)(T. Otsuka et al., Prog. Part. Nucl Phys. 46, 319 (2001)) which **samples** the relevant basis states stochastically
- **D**ensity **M**atrix **R**enormalization **G**roup (J. Dukelsky and S. Pittel, Rep. Prog. Phys. 67, 513 (2004)), borrowed from condensed matter physics (S. R. White PRL 69, 2863 (1992))

Direct diagonalization: Lanczos

- **Goal:** Construction of an orthonormal basis which renders **H tridiagonal**

- **Procedure**

1) Choice of a **pivot** (normalized) state **$|1\rangle$**

2) Action of **H** on **$|1\rangle$**

$$|a_1\rangle = H|1\rangle = |1\rangle H_{11} + |2'\rangle$$

$$\langle 1|2'\rangle = 0 \quad |2\rangle = |2'\rangle / \langle 2'|2'\rangle^{1/2}$$

3) Construction of **H_{ij}**

$$H_{11} = \langle 1|H|1\rangle = \langle 1|a_1\rangle$$

$$H_{12} = \langle 1|H|2\rangle = \langle a_1|2\rangle = \langle 2'|2'\rangle^{1/2}$$

Direct diagonalization: Lanczos

At the k -th step:

$$|a_k\rangle = H|k\rangle = H_{kk-1} |k-1\rangle + H_{kk} |k\rangle + |(k+1)'\rangle$$

- $H_{kk-1} = \langle k|H|k-1\rangle$
- $H_{kk} = \langle k|H|k\rangle = \langle k|a_k\rangle$
- $H_{kk+1} = \langle (k+1)'|(k+1)'\rangle^{1/2}$

The **iteration** stops as soon as

$$H_{kk+1} = \langle (k+1)'|(k+1)'\rangle^{1/2} = 0.$$

In practical cases when

$$H_{kk+1} = \langle (k+1)'|(k+1)'\rangle^{1/2} < \varepsilon$$

Direct diagonalization: Lanczos

- Generally very **efficient**: It handles matrices of $N \sim 10^6 \div 10^9$ (in the m-scheme)
- **Numerical problems** : The state vectors are **mathematically** but **not numerically orthogonal**: **spurious solutions may appear**

Stochastic SM Monte-Carlo (SMMC)

- **Main tool:** Imaginary time evolution operator

$$U = \exp(-\beta H) \quad (\beta = 1/T)$$

- **Property**

$$U |0\rangle \xrightarrow{\beta \rightarrow \infty} \Psi \quad (\text{true ground state})$$

$$\langle A \rangle = \langle 0 | U^\dagger A U | 0 \rangle \xrightarrow{\beta \rightarrow \infty} (\Psi, A \Psi)$$

- * **Goal:** Compute

$$\langle A \rangle = (1/Z) \text{Tr}(UA) \quad (\text{Tr}X = \sum \langle i | X | i \rangle)$$

$$Z = \text{Tr} U$$

Easy for a one body (unperturbed) Hamiltonian

$$U \phi = \phi'$$

$$\text{Tr}U = \det(1 + U)$$

Stochastic SM Monte-Carlo (SMMC)

- Preliminary operation

- $H = \sum \varepsilon_\alpha O_\alpha + \sum V_\alpha A_\alpha^\dagger A_\alpha$ ($A_\alpha = (a_i \otimes a_j)_\alpha$)
 $\rightarrow \sum \varepsilon_\alpha O_\alpha + \sum V_\alpha O_\alpha^\dagger O_\alpha$ ($O_\alpha = \sum c_{ij} (a_i^\dagger \otimes a_j)_\alpha$)

- Linearization (Hubbard-Stratonovich)

- Easy for $\alpha = 1$ (Gaussian identity)

$$\text{Exp}(-\beta H) = \int d\sigma e^{-(\beta|V|\sigma^2)/2} e^{-\beta h}$$

$$h = (\varepsilon + sV\sigma) O$$

- In the general case

$$[O_\alpha, O_\beta] \neq 0 \rightarrow e^{f(O_\alpha)+f(O_\beta)} \neq e^{f(O_\alpha)} e^{f(O_\beta)}$$

Stochastic SM Monte-Carlo (SMMC)

- In the general case

*Split β into N time slices of length $\Delta\beta = \beta/N$

$$\rightarrow U = U_N \dots U_{n+1} \dots U_1 = [e^{-\Delta\beta H}]^N$$

** For each slice n perform a linearization (Hubbard-Stratonovich) using auxiliary fields $\sigma_{\alpha n}$

$$\rightarrow \langle A \rangle = (1 / \int D\sigma W_\sigma) \int D\sigma W_\sigma A_\sigma$$

$$D\sigma = \prod_n \prod_\alpha d\sigma_{\alpha n} d\sigma_{\alpha n}^* (\Delta\beta |V_\alpha| / 2\pi)$$

$$W_\sigma = e^{-\Delta\beta \sum (V_\alpha \sigma^2)} \text{Tr} U_\sigma$$

$$A_\sigma = (\text{Tr} U_\sigma A) / \text{Tr} U_\sigma$$

$$U_\sigma = U_N \dots U_{n+1} U_1 \quad U_n = e^{-\Delta\beta h_n}$$

Stochastic SM Monte-Carlo (SMMC)

- Dimension D of integrals: $N_s^2 N$ (exceeds 10^5)
- Tools for evaluating the integrals: Montecarlo

Recast 

i) $\langle A \rangle = \int d^D \sigma P_\sigma A_\sigma$

$$P_\sigma = W_\sigma / \int d^D \sigma W_\sigma \equiv \text{probability weight} \quad \left(\int d^D \sigma P_\sigma = 1 \right)$$

$$P_\sigma \geq 0$$

ii) σ_s ($s=1, \dots, S$) be a set of randomly chosen S fields of weight P_σ

iii) $\langle A \rangle = \int d^D \sigma P_\sigma A_\sigma \approx (1/S) \sum_s A_s,$

$\langle A \rangle$ itself is a random variable \rightarrow Its average yields the required value.

iv) To estimate the uncertainties we invoke the Central limit theorem

$$\sigma_{\langle A \rangle}^2 = (1/S) \int d^D \sigma P_\sigma (A_\sigma - \langle A \rangle)^2 \approx (1/S^2) \sum_s (A_s - \langle A \rangle)^2$$

Stochastic SM Monte-Carlo (SMMC)

Generation of σ

(Metropolis, Rosenbluth, Rosenbluth, Teller):

Random-walk moving through σ -space

If the **walker** is at σ_k , to **generate** σ_{k+1} make a **trial step** at σ_t $\sigma_k \rightarrow \sigma_t$

Compute:

$$r = W_t / W_k$$

if $r > \varepsilon$ $\rightarrow \sigma_{k+1} = \sigma_t$ Otherwise σ_t is discarded

Stochastic SM Monte-Carlo (SMMC)

- It computes the **g.s. expectation values** of A
- It gives information on the **dynamical response**

$$R(\tau) = \langle A^\dagger(\tau) A(0) \rangle = \int e^{-\tau E} S(E) dE$$

(Laplace transform of the)

Strength function



$$S(E) = (1/Z) \sum_{if} e^{-\beta E_i} |\langle f|A|i\rangle|^2 \delta(E - E_f + E_i)$$

- it yields the **energy-weighted moments** of S

$$m_n = (1/Z) \sum_{if} e^{-\beta E_i} |\langle f|A|i\rangle|^2 (E_f - E_i)^n$$

- For **collective** states (exhausting most of the **strength**)
it estimates the **centroid** of the response

Stochastic SM Monte-Carlo (SMMC)

- No detailed spectroscopic information
- Sign problem

$$\langle A \rangle = \int d^D\sigma P_\sigma A_\sigma \quad (P_\sigma = W_\sigma / \int d^D\sigma W_\sigma)$$

$$\int d^D\sigma P_\sigma = 1 \quad P_\sigma \geq 0$$

$$\rightarrow W_\sigma \geq 0$$

- This is the case only if all $V_\alpha \leq 0$

true for schematic Hamiltonians (pairing plus quadrupole), but not for realistic Hamiltonians!

Quantum Monte-Carlo Diagonalization (QMCD)

- It states a **bridge** between **SMMC** and **direct diagonalization**: It searches stochastically the basis states using the previous method
- Split β into N time slices of length $\Delta\beta = \beta/N$
 $\rightarrow U = U_N \dots U_{n+1} U_n \dots U_1 = \prod_n e^{-\Delta\beta H}$
- For each slice n perform a linearization (Hubbard-Stratonovich) using **auxiliary fields** $\sigma_{\alpha n}$
 $\rightarrow U \approx \int D\sigma e^{-\Delta\beta \sum_{\alpha} (V_{\alpha} \sigma_{\alpha n}^2)} \prod_n e^{-\Delta\beta h_n}$
- $D\sigma = \prod_n \prod_{\alpha} d\sigma_{\alpha n} d\sigma_{\alpha n}^* (\Delta\beta |V_{\alpha}| / 2\pi)$

Quantum Monte-Carlo Diagonalization (QMCD)

i) Generates stochastically a set of auxiliary fields

$\sigma = \{\sigma_1 \dots \sigma_n \dots \sigma_N\}$ obtaining the QMC basis states

$$\Phi(\sigma) \propto \prod_n e^{-\Delta\beta h(\sigma_n)} \Psi(0) \quad (1)$$

for different sets σ . $\Psi(0)$ is a Slater determinat.

ii) Diagonalize H in the space spanned by the states so generated.

iii) Suppose now that one has generated the basis states

$$\Phi_1 \dots \Phi_n$$

iv) Using Eq. (1) one generates an additional basis state $\Phi_{n+1} = \Phi(\sigma)$ and diagonalize H in the space spanned by

$$\Phi_1 \dots \Phi_n \Phi_{n+1}$$

v) If the diagonalization lowers appreciably the energy eigenvalue, $\Phi(\sigma)$ is adopted, otherwise is discarded.

The iteration stops until convergence toward a given set of lowest eigenvalues is attained.

Quantum Monte-Carlo Diagonalization (QMCD)

i) Generates stochastically a set of auxiliary fields

$\sigma = \{\sigma_1 \dots \sigma_n \dots \sigma_N\}$ obtaining the QMC basis states

$$\Phi(\sigma) \propto \prod_n e^{-\Delta\beta h(\sigma_n)} \Psi(0) \quad (1)$$

for different sets σ . $\Psi(0)$ is a Slater determinant.

ii) Diagonalize H in the space spanned by the states so generated.

iii) Suppose now that one has generated the basis states

$$\Phi_1 \dots \Phi_n$$

iv) Using Eq. (1) one generates an additional basis state $\Phi_{n+1} = \Phi(\sigma)$ and diagonalize H in the space spanned by

$$\Phi_1 \dots \Phi_n \Phi_{n+1}$$

v) If the diagonalization lowers appreciably the energy eigenvalue, $\Phi(\sigma)$ is adopted, otherwise is discarded.

The iteration stops until convergence toward a given set of lowest eigenvalues is attained.

Quantum Monte-Carlo Diagonalization (QMCD)

- The states are to be orthogonalized
- M (and J) projection is needed
- Redundancy is to be removed
- **On the other hand** it has the advantages of SM : It allows an explicit study of the wave functions while reducing drastically the dimensions of standard SM.

Focus on : direct methods for finding extremal eigenvalues - 1

Symmetric/Hermitian eigenvalue problem:

$$A\mathbf{x} = \lambda M\mathbf{x}, \quad A = A^*, \quad M = M^* > 0.$$

Direct, iterative methods are generally based on the minimization of the Rayleigh quotient:

$$\lambda_1 = \min_{\mathbf{x} \neq \mathbf{0}} \rho(\mathbf{x}) \quad \rho(\mathbf{x}) = \frac{\mathbf{x}^* A \mathbf{x}}{\mathbf{x}^* M \mathbf{x}}$$

The idea is to find a sequence of vectors \mathbf{x}_k for which :

$$\rho(\mathbf{x}_{k+1}) < \rho(\mathbf{x}_k)$$

The hope is that the corresponding sequence of ρ converges to λ_1 , and by consequence \mathbf{x}_k to the first eigenvector

Focus on : direct methods for finding extremal eigenvalues - 2

Convergence has been shown for almost all the starting vectors (see B. N. Parlett & W. Kahan, "On the convergence of a practical QR algorithm. (With discussion)," Information Processing, 68 and J. H. Wilkinson, "Global convergence of tridiagonal QR algorithm with origin shifts," Linear Algebra and Appl, 1)

Iteration are based on the definition of a "search direction" :

$$\mathbf{x}_{k+1} = \mathbf{x}_k + \delta_k \mathbf{p}_k$$

Where the parameter is variationally determined :

$$\rho(\mathbf{x}_{k+1}) = \min_{\delta} \rho(\mathbf{x}_k + \delta \mathbf{p}_k)$$

Generalized Optimal Relaxation Method (ORM) - 1

A generalization of the ORM consist in diagonalizing the Hamiltonian in the space spanned by \mathbf{x}_k and the basis vector \mathbf{e}_i

$$\begin{pmatrix} \langle \mathbf{x}_k | H | \mathbf{x}_k \rangle & \langle \mathbf{x}_k | H | \mathbf{e}_i \rangle \\ \langle \mathbf{e}_i | H | \mathbf{x}_k \rangle & \langle \mathbf{e}_i | H | \mathbf{e}_i \rangle \end{pmatrix} = \begin{pmatrix} \lambda_1 & b_i \\ b_i & a_{ii} \end{pmatrix}$$

It is a “generalization” for two main reasons :

1) Convergence is assured by the weak separation property of the matrix eigenvalues :

$$\lambda'_1 \leq \lambda_1 \leq \lambda'_2$$

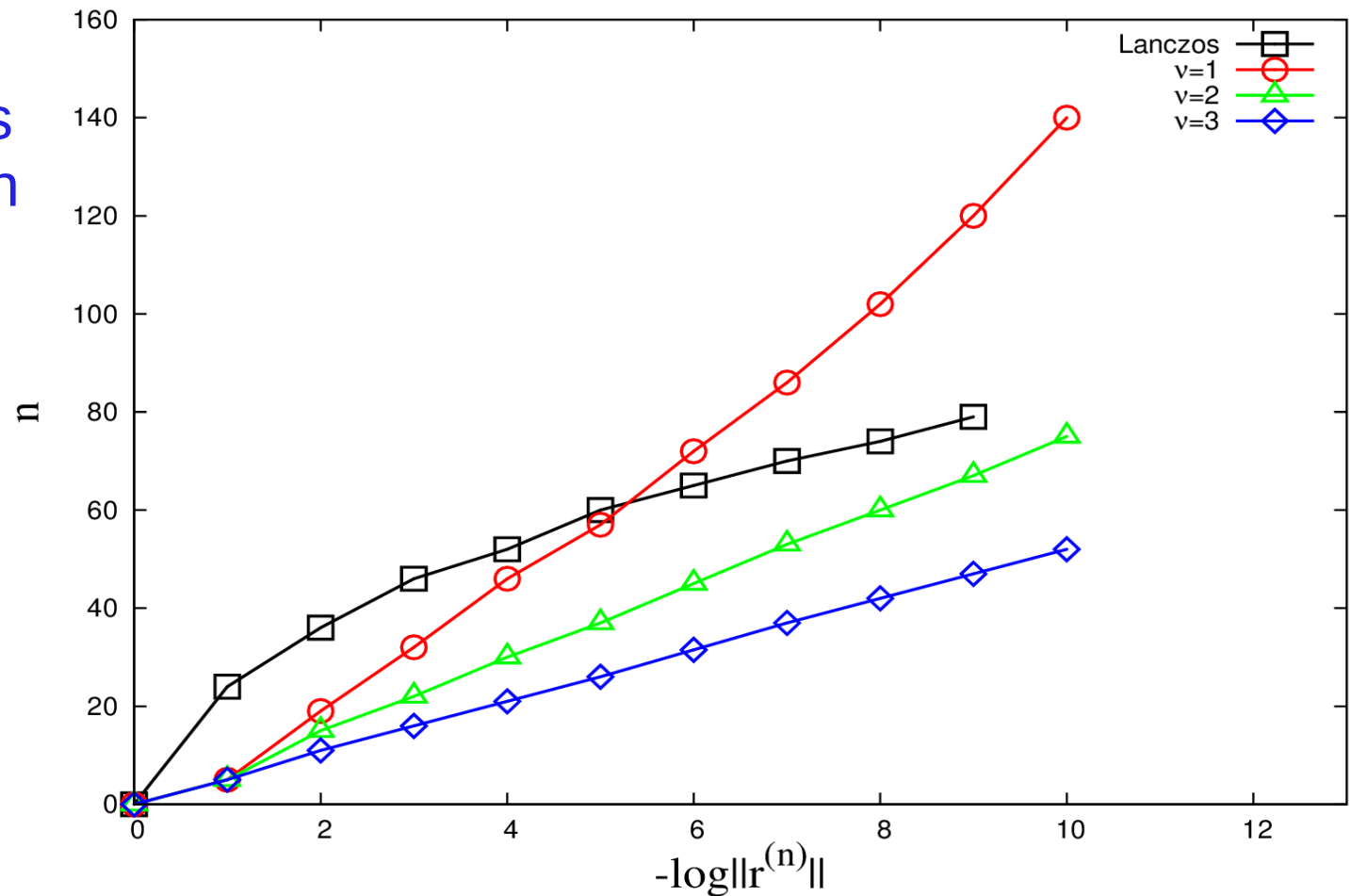
2) It can include more eigenvalues:

$$\begin{pmatrix} \lambda_1 & 0 & 0 & b_{1i} \\ 0 & \lambda_2 & 0 & b_{2i} \\ 0 & 0 & \lambda_3 & b_{3i} \\ b_{1i} & b_{2i} & b_{3i} & a_{ii} \end{pmatrix}$$

Generalized Optimal Relaxation Method (ORM) - 2

Its convergence properties can be assessed against the Lanczos algorithm (ARPACK package) using a finite difference matrix deduced from Laplace equation :

Its main advantage is that it can be used on normal machines for performing Large Scale Shell Model calculations



Generalized Optimal Relaxation Method (ORM) - 3

The algorithm is based on the **diagonalization** of a matrix, which in practice can be **avoided**

A **similarity** transformation allows to determine the **v+1 eigenvalues** by solving the **dispersion relation**
(**Sampling condition**)

$$\Delta\lambda = \sum_j \Delta\lambda_j = \sum_{i=1,v} | \lambda_i' - \lambda_i | = \sum_j b_j^2 / (a_{jj} - \lambda - \Delta\lambda_j)$$

which is of the type **f(z) = z**, fulfilling the condition

$$1 - d/dz(f) > 0$$

It is of **easier** and **faster** solution (**Newton** method of **derivatives**)

Generalized Optimal Relaxation Method (ORM) - 4

We have then derived the endowed sampling criterion. The leading term in the difference of two eigenvalues is given by:

$$|\langle \mathbf{x}_k^{(i-1)} | \mathbf{H} | j \rangle|^2 / (a_{jj} - \lambda_k^{(i-1)}) > \varepsilon_i$$

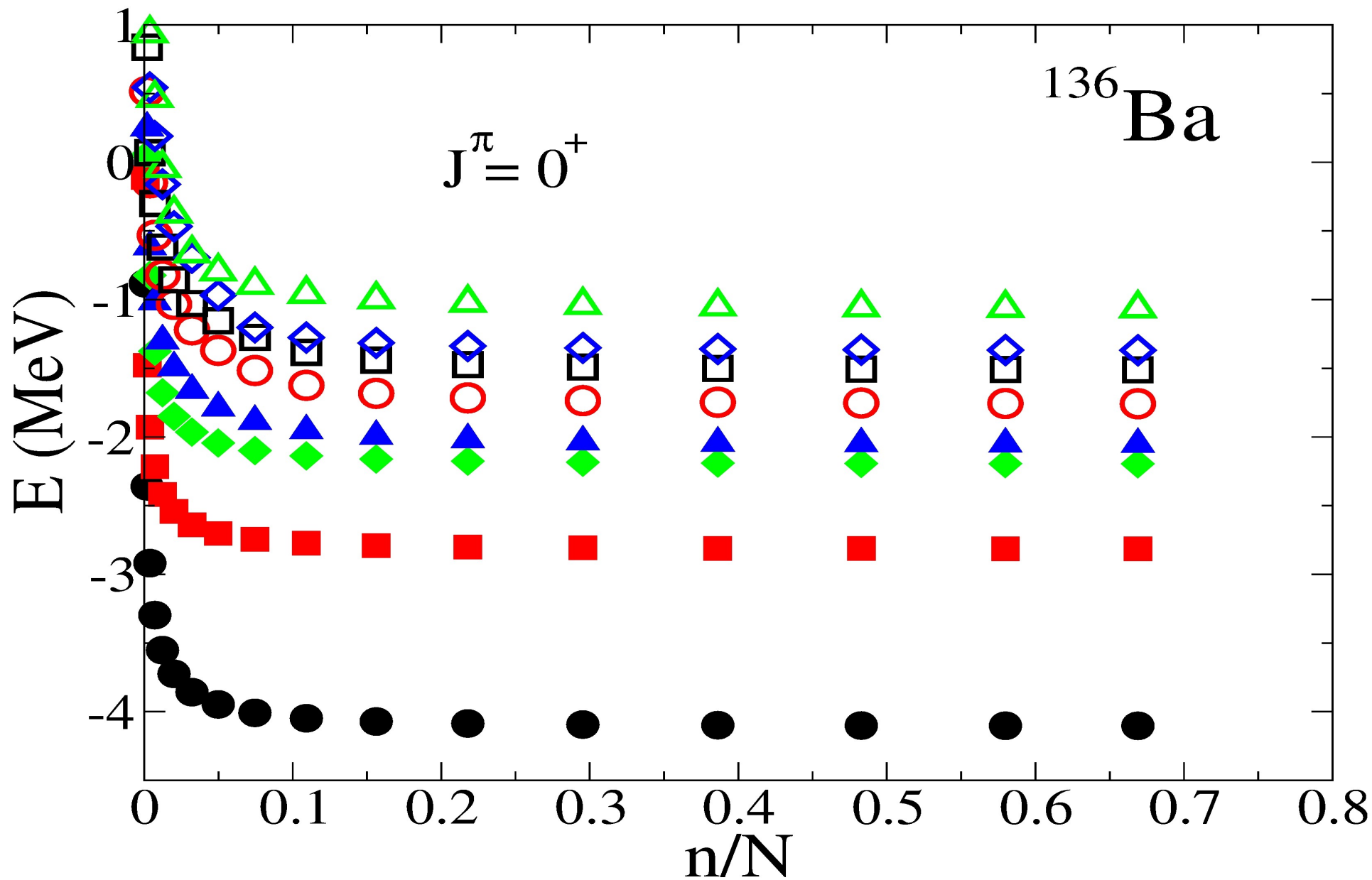
Since the method induces a space decomposition :

$$\mathbf{I} = \mathbf{M}_0 \oplus \mathbf{M}_1 \oplus \dots \oplus \mathbf{M}_p$$

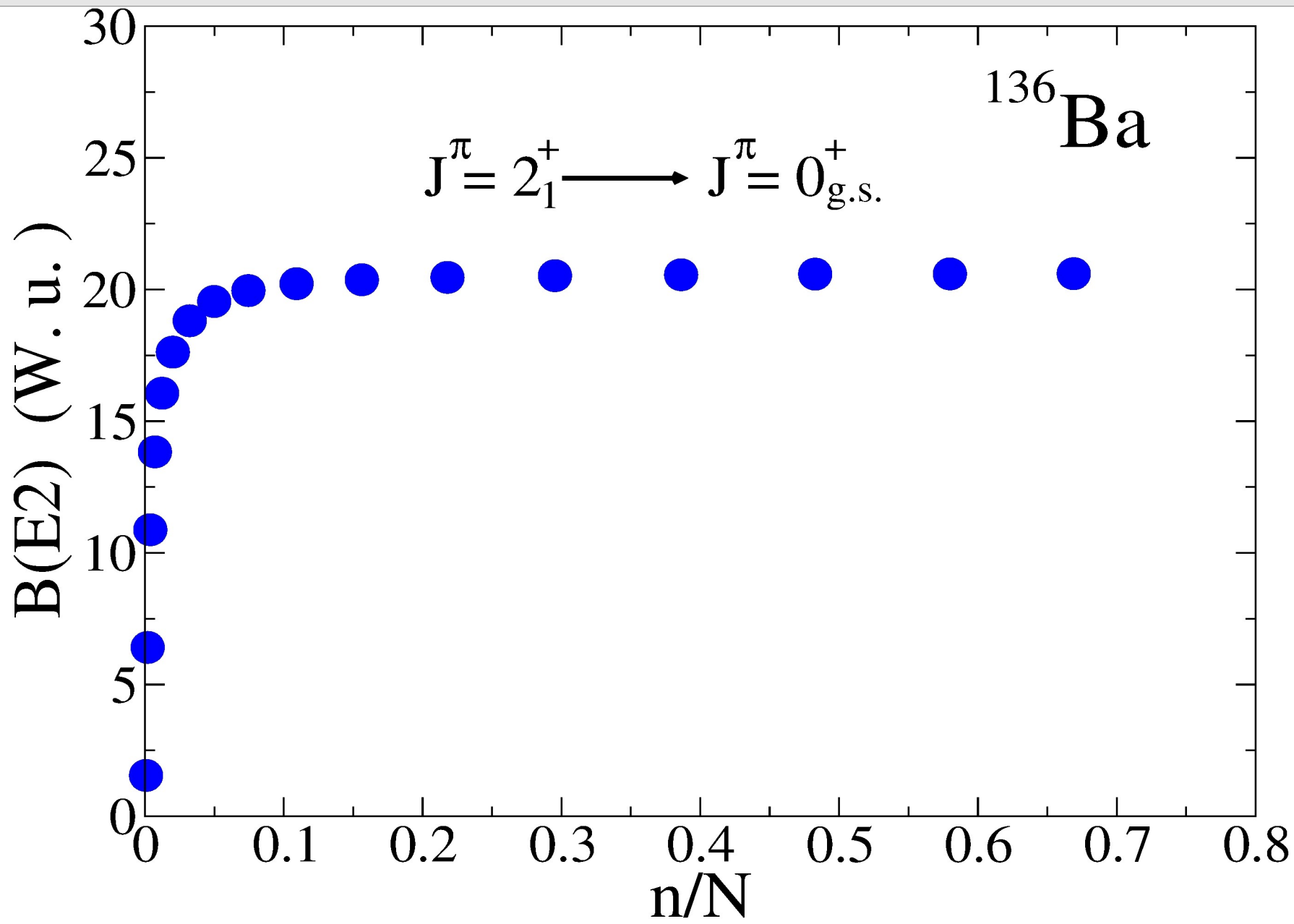
We start with an exact diagonalization in \mathbf{M}_0 , and then sample the subspaces connected by the Hamiltonian with increasingly smaller thresholds:

$$\varepsilon_1 > \varepsilon_2 > \dots > \varepsilon_{p-1} > \varepsilon_p$$

Generalized Optimal Relaxation Method (ORM) - 4



Generalized Optimal Relaxation Method (ORM) - 5



Collectivity in nuclei - 1

Historically, two models constitute the main examples of collectivity in nuclei, being supported by strong experimental evidences:

- (Harmonic Quadrupole) vibrator model
- (Rigid) rotor model

Of course, they do not exhaust all the possible collective pictures of nuclei, but rather represent two “extremal” situations, as can be simply understood in term of semi-classical models

Vibrations about a spherical shape

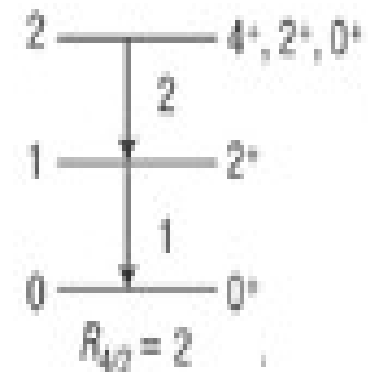
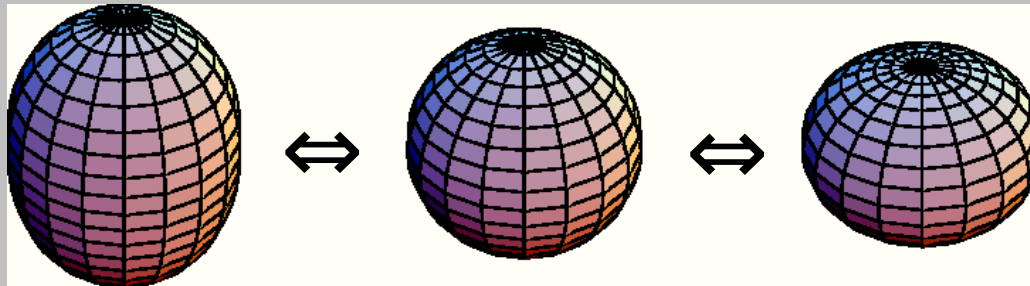
Vibrations are characterized by a multipole quantum number λ in surface parametrization:

$$R(\theta, \phi) = R_0 \left(1 + \sum_{\lambda} \sum_{\mu=-\lambda}^{+\lambda} \alpha_{\lambda\mu} Y_{\lambda\mu}^*(\theta, \phi) \right)$$

$\lambda=0$: compression (high energy)

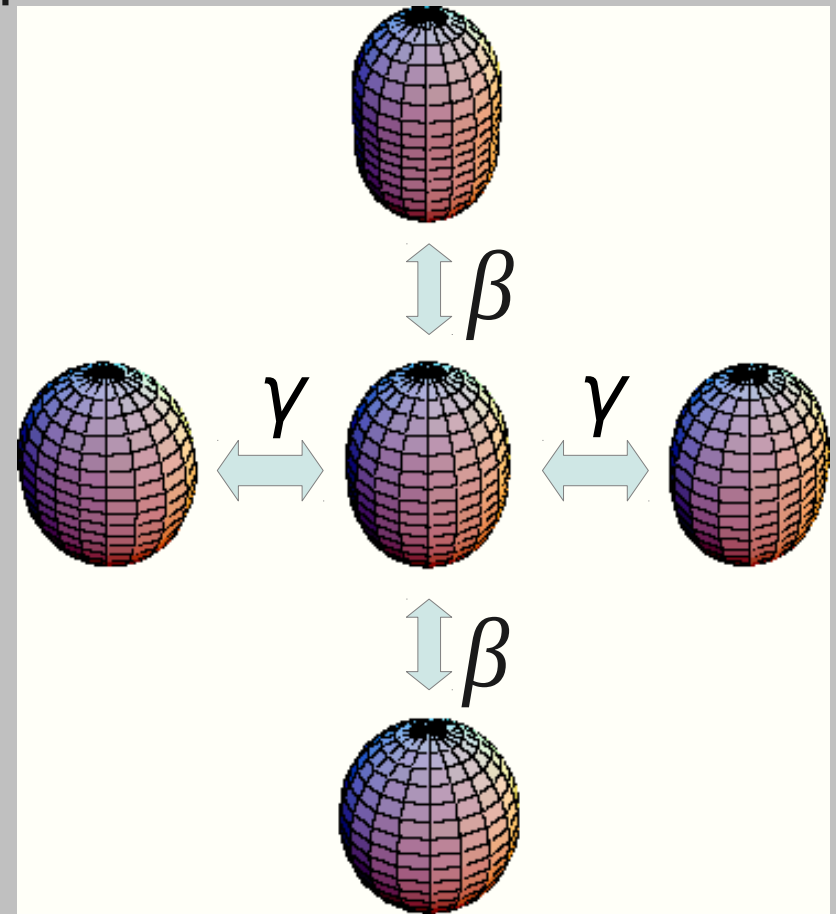
$\lambda=1$: translation (not an intrinsic excitation)

$\lambda=2$: quadrupole vibration



Vibrations about a spheroidal shape

- The vibration of a shape with axial symmetry is characterized by $\alpha_{\lambda\mu}$.
- Quadrupole oscillations:
 - $\mu=0$: along the axis of symmetry (β)
 - $\mu=\pm 1$: spurious rotation
 - $\mu=\pm 2$: perpendicular to axis of symmetry (γ)

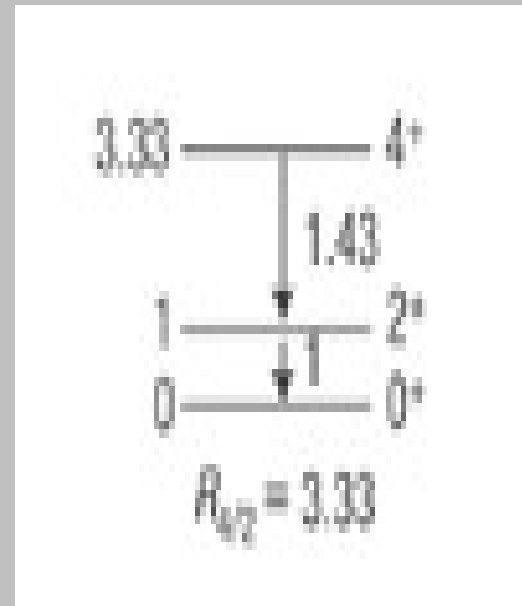


Rigid Rotor

- Hamiltonian of quantum mechanical rotor in terms of 'rotational' angular momentum R :

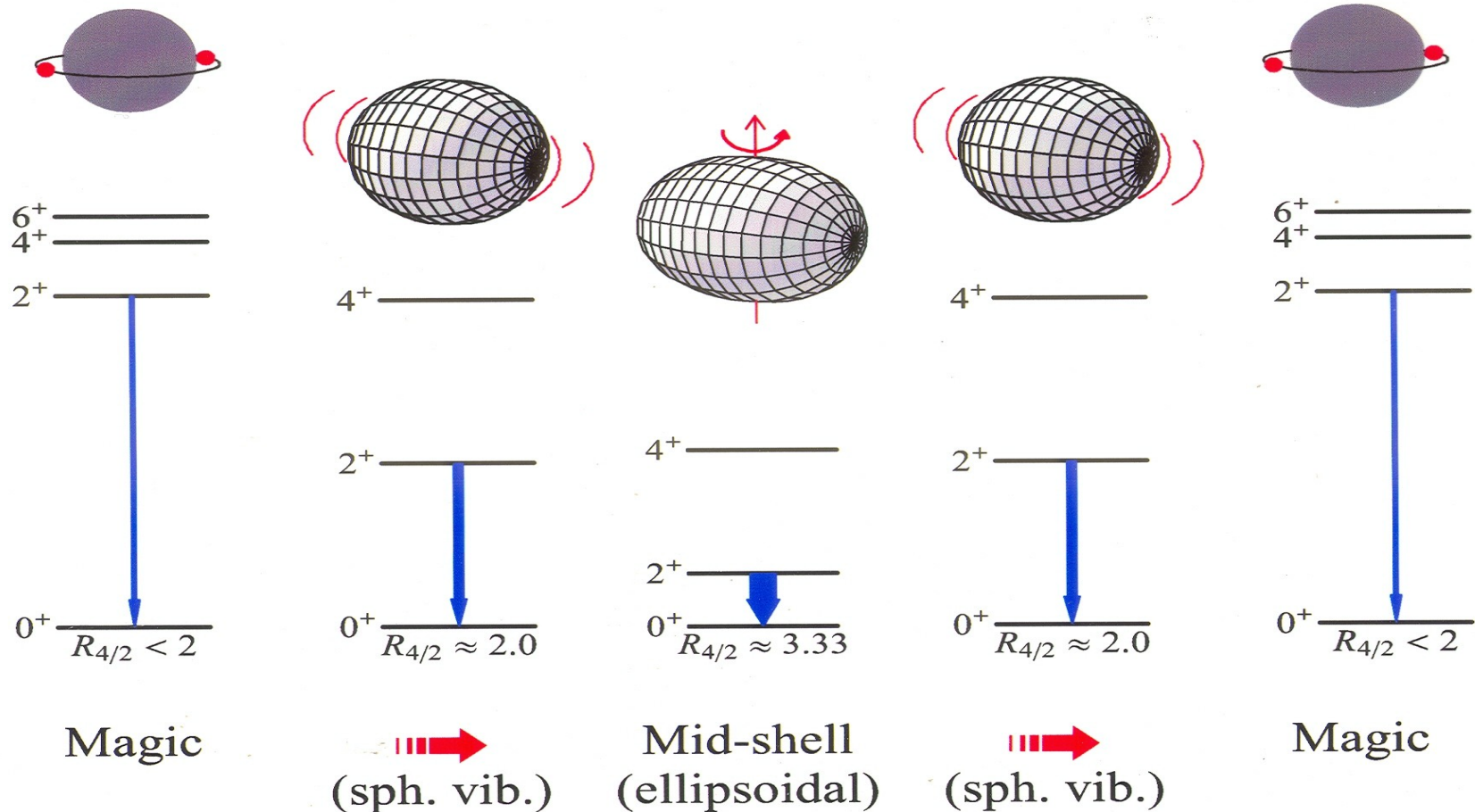
$$\hat{H}_{\text{rot}} = \frac{\hbar^2}{2} \left[\frac{R_1^2}{\mathfrak{J}_1} + \frac{R_2^2}{\mathfrak{J}_2} + \frac{R_3^2}{\mathfrak{J}_3} \right] = \frac{\hbar^2}{2} \sum_{i=1}^3 \frac{R_i^2}{\mathfrak{J}_i}$$

- Nuclei have an additional intrinsic part H_{intr} with 'intrinsic' angular momentum J .
- The total angular momentum is $I = R + J$.



Collectivity between two closed shells

Evolution of nuclear structure (as a function of nucleon number)



The Interacting Boson Model (IBM)

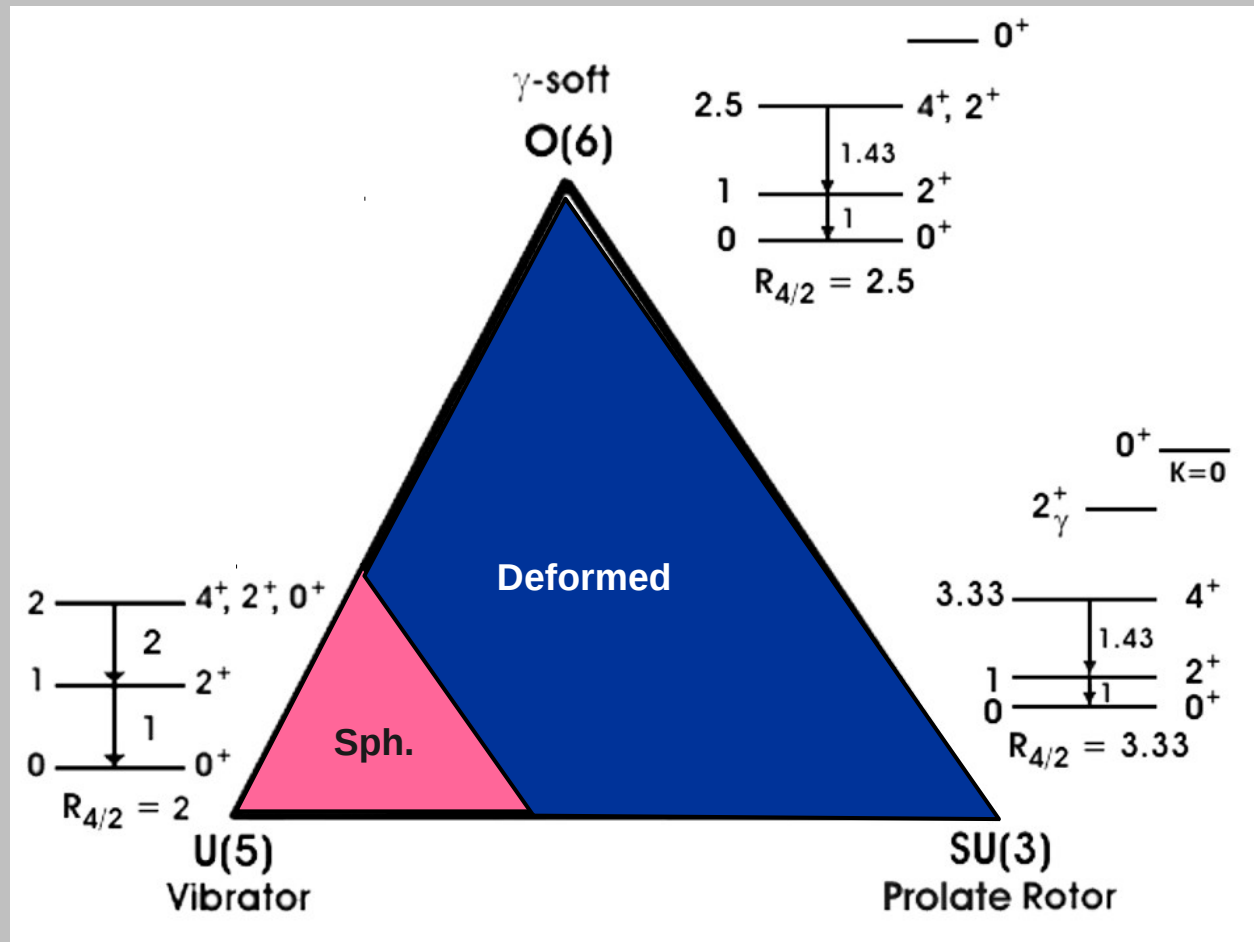
- Nuclear collective excitations are described in terms of N s and d bosons.
- Spectrum generating algebra for the nucleus is $U(6)$. All physical observables (hamiltonian, transition operators,...) are expressed in terms of the generators of $U(6)$.
- Formally, nuclear structure is reduced to solving the problem of N interacting s and d bosons.
- Rotational invariant hamiltonian with up to N -body interactions (usually up to 2):

$$H_{\text{IBM}} = \varepsilon_s n_s + \varepsilon_d n_d + \sum_{ijkl} v_{ijkl}^L (b_i^+ \times b_j^+)^{(L)} \cdot (\tilde{b}_k \times \tilde{b}_l)^{(L)}$$

- Finding exactly-solvable form of the Hamiltonian is equivalent to enumerate the $U(6)$ sub-models:

$$U(6) \supset G \supset SO(3)$$

Symmetry Triangle



Most nuclei do not exhibit the idealized symmetries but rather lie in transitional regions.

Mixed-symmetry states - 1

Proton neutron mixed-symmetry states can be correctly understood in the framework of the proton-neutron version of the Interacting Boson Model, or IBM-2.

An alternate, semi-quantitative way to introduce them is using the so-called Q-phonon scheme, introduced by Otsuka in the '90 (roughly speaking, only d-bosons are taken into account).

Q-phonon scheme has the advantage of being more intuitively related to the physics of the system, even if it assumes a good F-spin quantum number. F-spin is a bosonic analogue to isospin, and is used to distinguish between proton and neutron bosons.

Mixed-symmetry states - 2

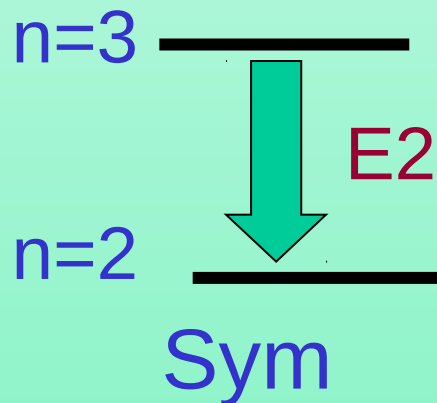
Symmetric States

$$|n, \nu\rangle_s = Q_s^n |0\rangle = (Q_p + Q_n)^n |0\rangle$$

Signature:

$$M(E2) \propto Q_s \quad (\Delta n = 1)$$

symmetry preserving
($\Delta F = 0$)



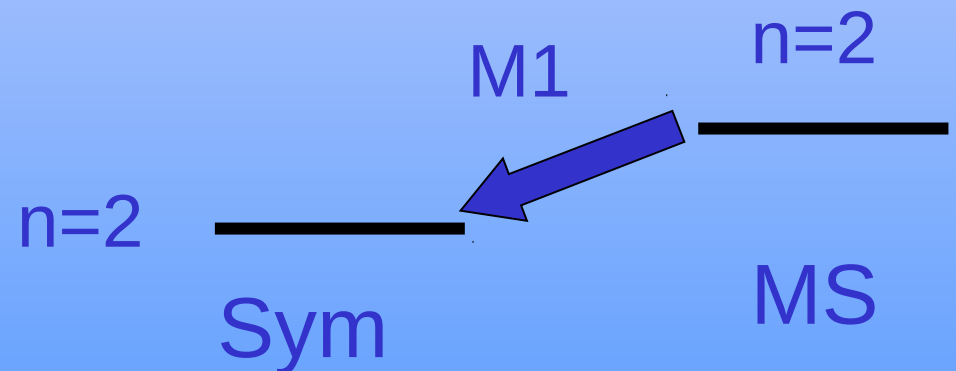
MS States

$$|n, \nu\rangle_{MS} = (Q_p - Q_n)(Q_p + Q_n)^{(n-1)} |0\rangle$$

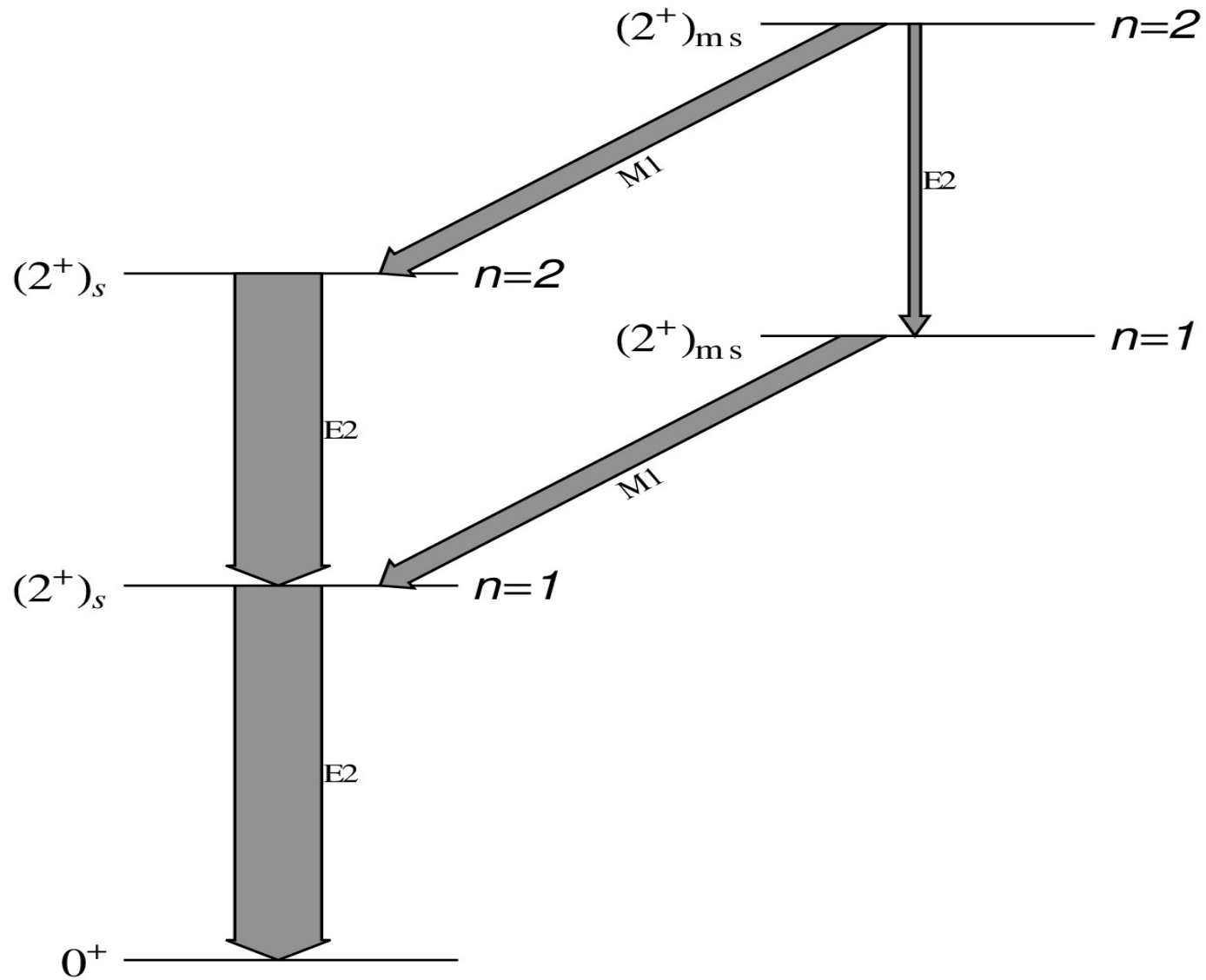
Signature

$$M(M1) \propto J_n - J_p \quad (\Delta n = 0)$$

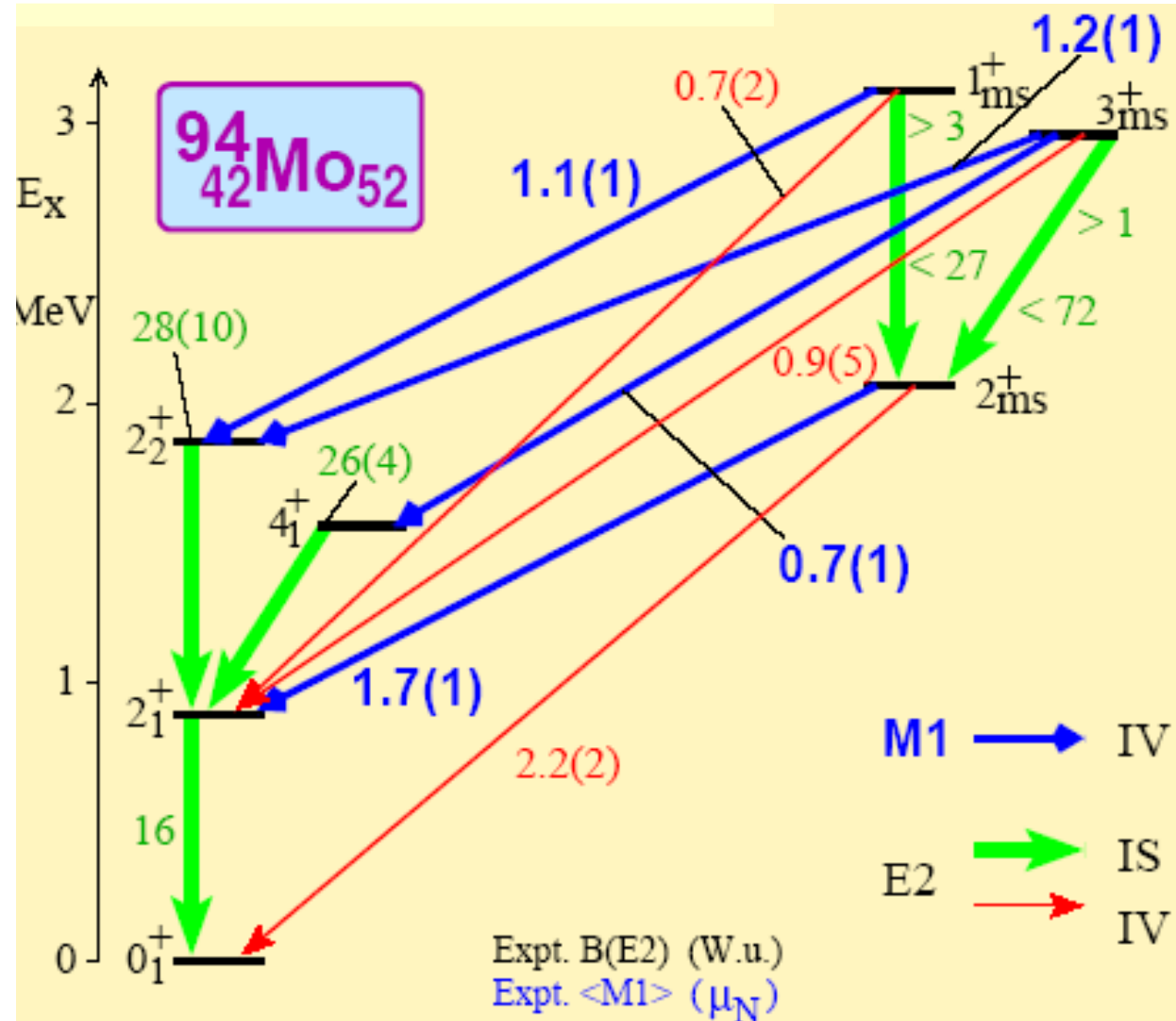
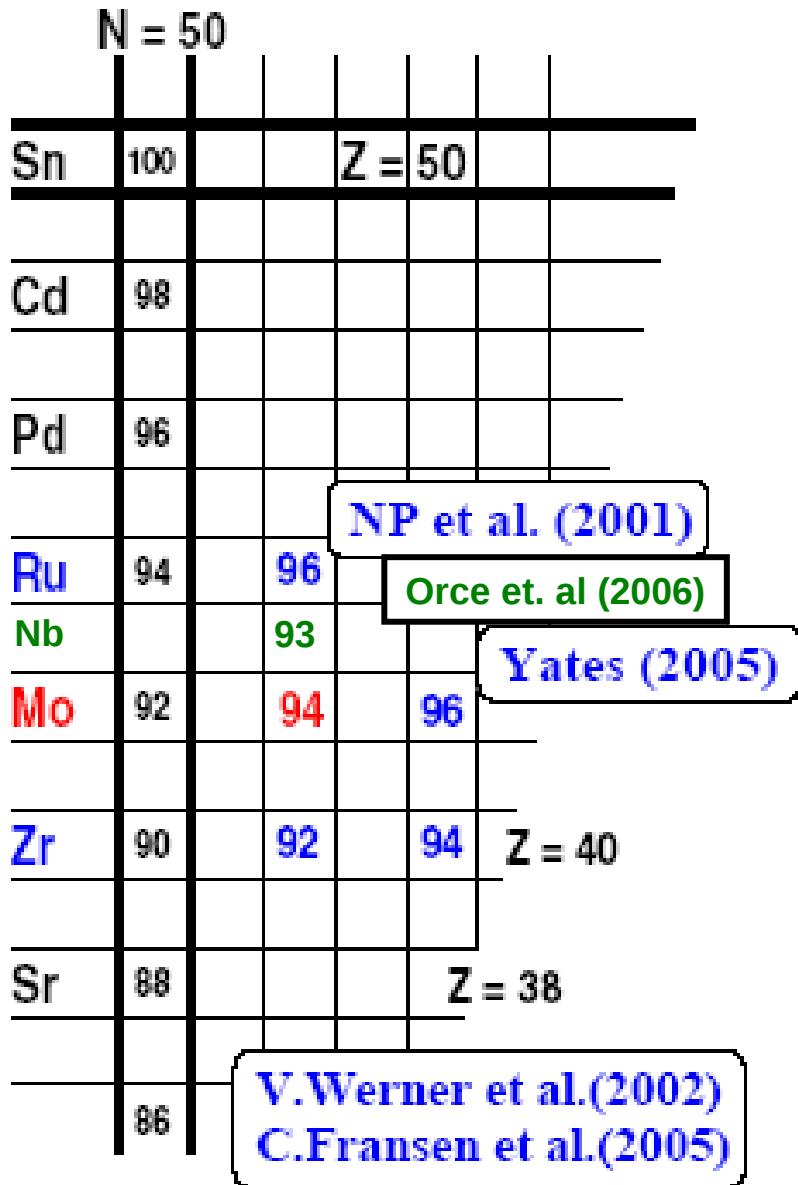
symmetry changing ($\Delta F = 1$)



Mixed-symmetry states - 3



Experimental evidence of MSS



N. Pietralla, C. Fransen et al., Phys. Rev. Lett. 83, 1303 (1999).
 N. Pietralla, C. Fransen et al., Phys. Rev. Lett. 84, 3775 (2000).
 C. Fransen, N. Pietralla et al., Phys. Rev. C 67, 024307 (2003).

MSS as Scissors excitations

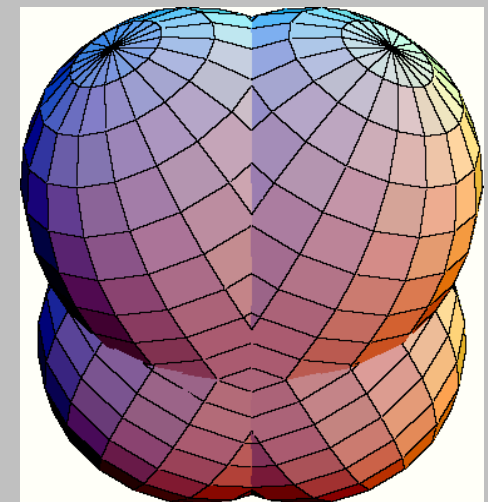
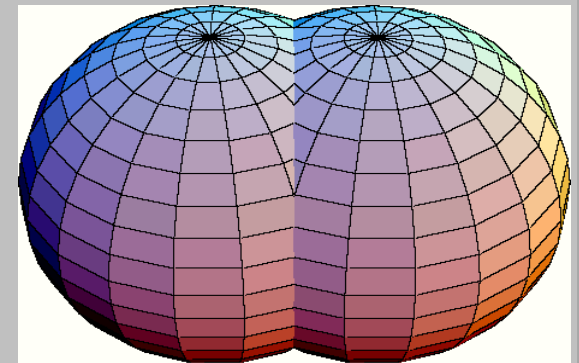
Collective displacement modes between neutrons and protons:

- *Linear* displacement (giant dipole resonance):

$$R_{\nu}-R_{\pi} \Rightarrow E1 \text{ excitation.}$$

- *Angular* displacement (scissors resonance):

$$L_{\nu}-L_{\pi} \Rightarrow M1 \text{ excitation.}$$



N. Lo Iudice & F. Palumbo, Phys. Rev. Lett. **41** (1978) 1532
F. Iachello, Phys. Rev. Lett. **53** (1984) 1427
D. Bohle *et al.*, Phys. Lett. B **137** (1984) 27

Collectivity and Shell Model

Large scale Shell Model calculations have been used for probing the collectivity of medium-heavy nuclei below and above the double shell-closure corresponding to ^{132}Sn ($Z=50$, $N=82$)

As we will see, signature for proton-neutron mixed-symmetry states has been correctly reproduced for isotopes described in terms of neutron holes, whether it seems to disappear moving towards the neutron drip line.

Calculation details - 1

Single proton-particle and neutron-hole energies (in MeV); We used the levels of ^{135}Xe as neutron single-hole energies, while for the protons, we took the single-particle energies adopted in a previous work for studying ^{133}Xe

$(nlj)_\pi$	$2d_{5/2}$	$1g_{7/2}$	$3s_{1/2}$	$2d_{3/2}$	$1h_{11/2}$
ϵ_p	0.00	0.2	2.2	2.3	2.9
$(nlj)_\nu^{-1}$	$(2d_{3/2})^{-1}$	$(3s_{1/2})^{-1}$	$(1h_{11/2})^{-1}$	$(1g_{7/2})^{-1}$	$(2d_{5/2})^{-1}$
ϵ_n	0.00	0.2885	0.5266	1.1315	1.2604

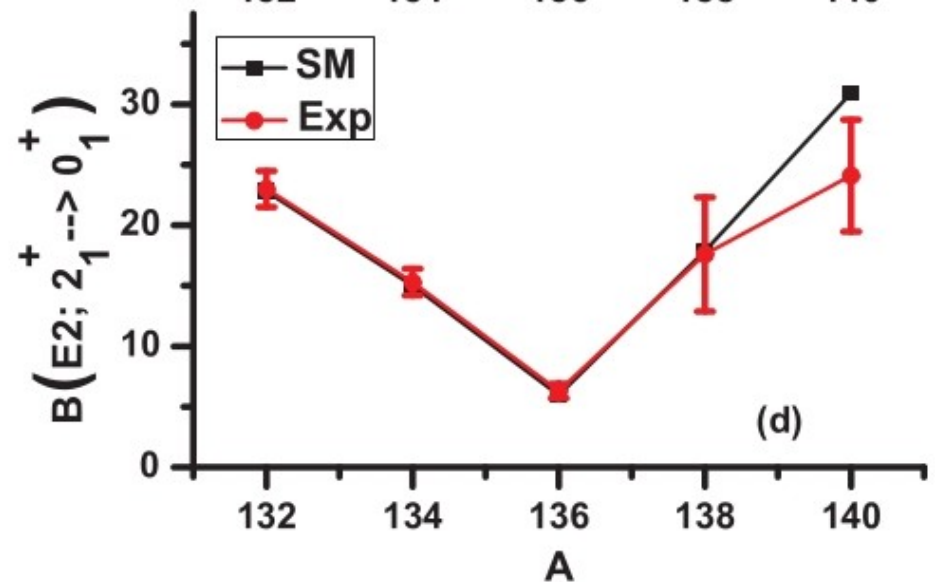
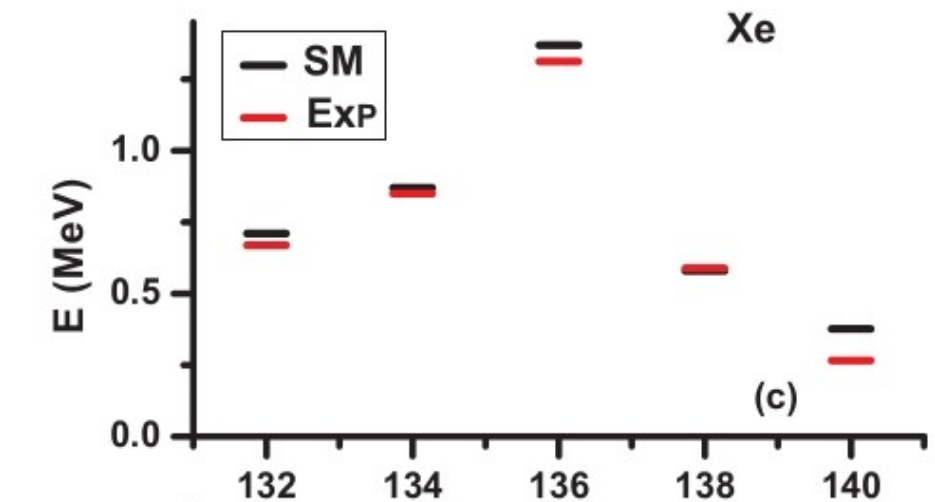
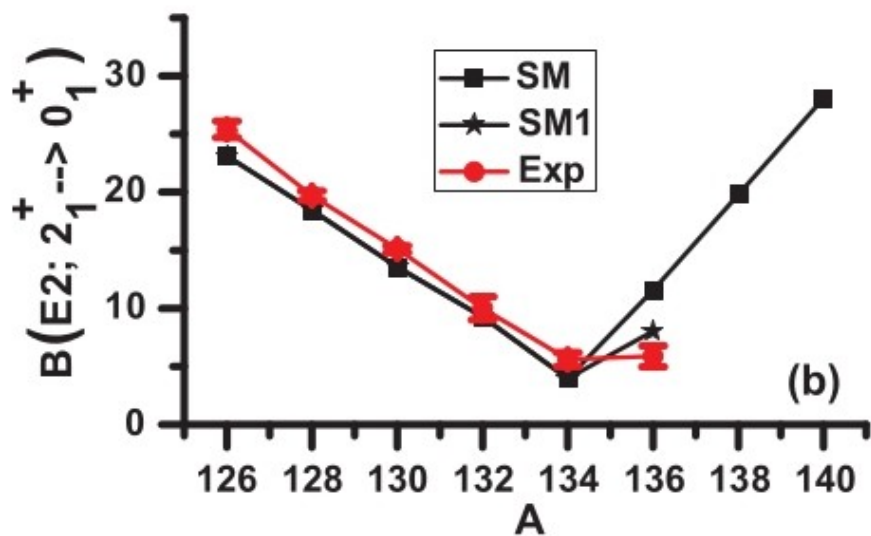
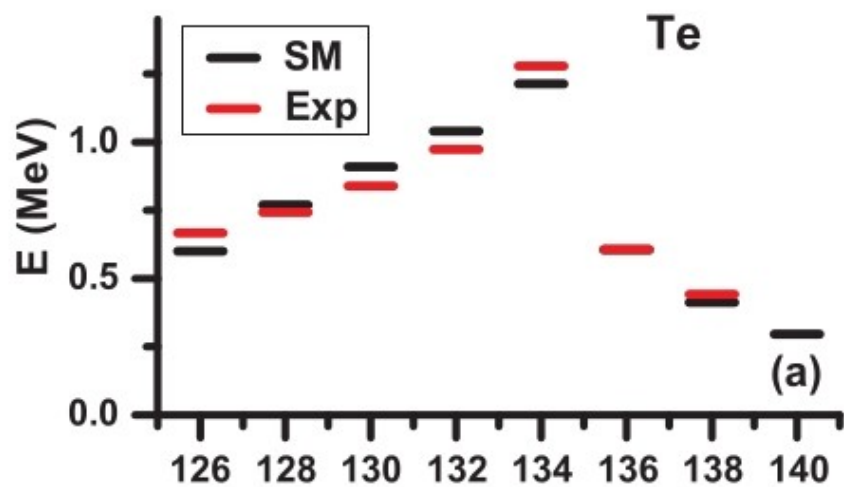
Calculation details - 2

Single proton- and neutron-particle energies (in MeV); We used the levels of ^{133}Sn for the neutrons and those of ^{133}Sb for protons, with minor modifications for reproducing energy spectra and transition strength of ^{134}Sn and ^{134}Te

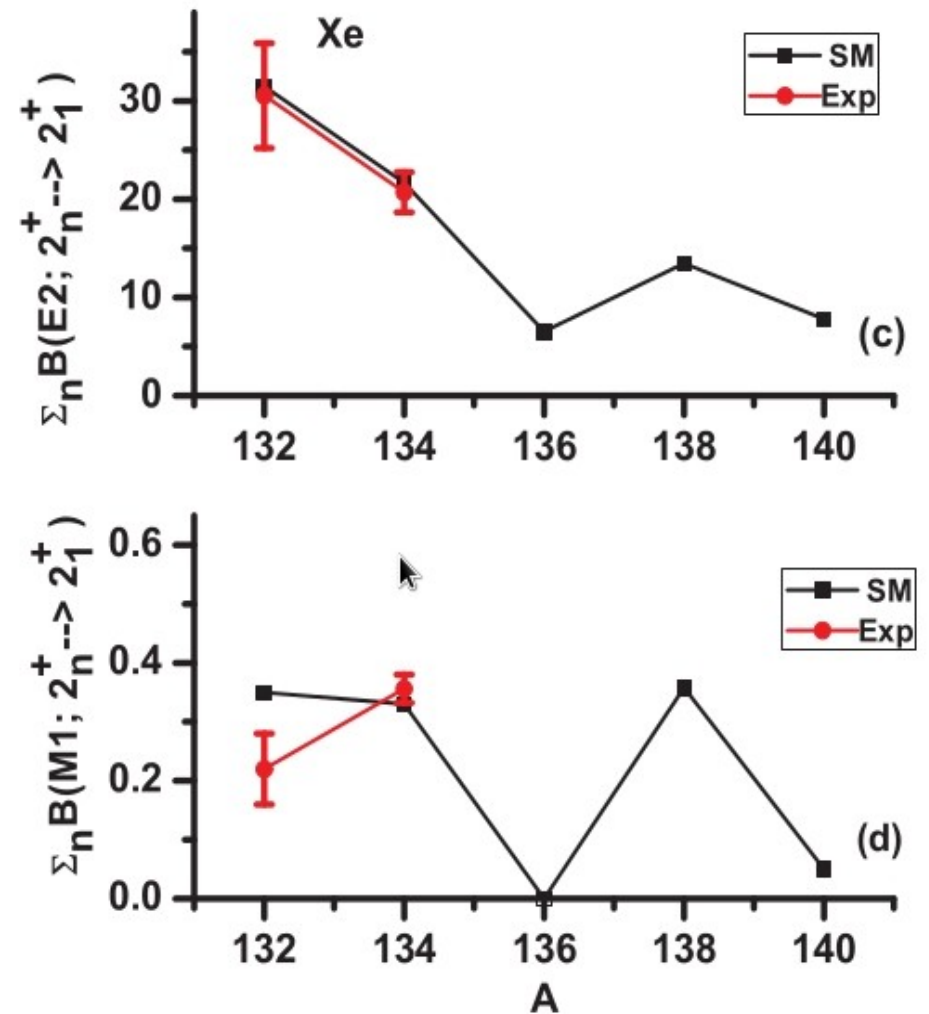
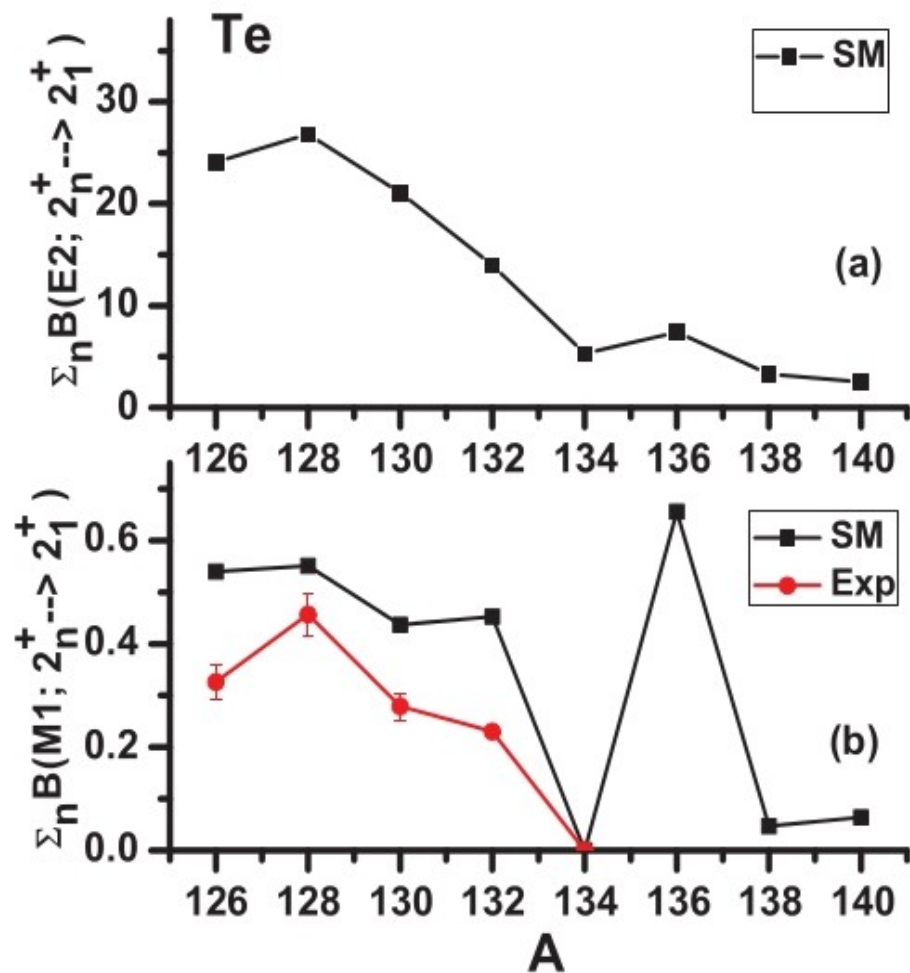
$(nlj)_\pi$	$1g_{7/2}$	$2d_{5/2}$	$2d_{3/2}$	$1h_{11/2}$	$3s_{1/2}$	
ϵ_π	0.00	0.96	2.71	2.80	3.5	
$(nlj)_\nu$	$2f_{7/2}$	$3p_{3/2}$	$1h_{9/2}$	$3p_{1/2}$	$2f_{5/2}$	$1i_{13/2}$
ϵ_ν	0.00	0.85	1.56	1.66	2.00	2.11

Moreover, these optimizations have also required a scaling by factors 1.1 and 1.2, respectively, of the $J^\pi = 0^+$ proton-proton and neutron-neutron pairing-like components of the two-body potential.

Te and Xe Isotopes towards drip lines - 1



Te and Xe Isotopes towards drip lines - 2



Tellurium isotopes - 1

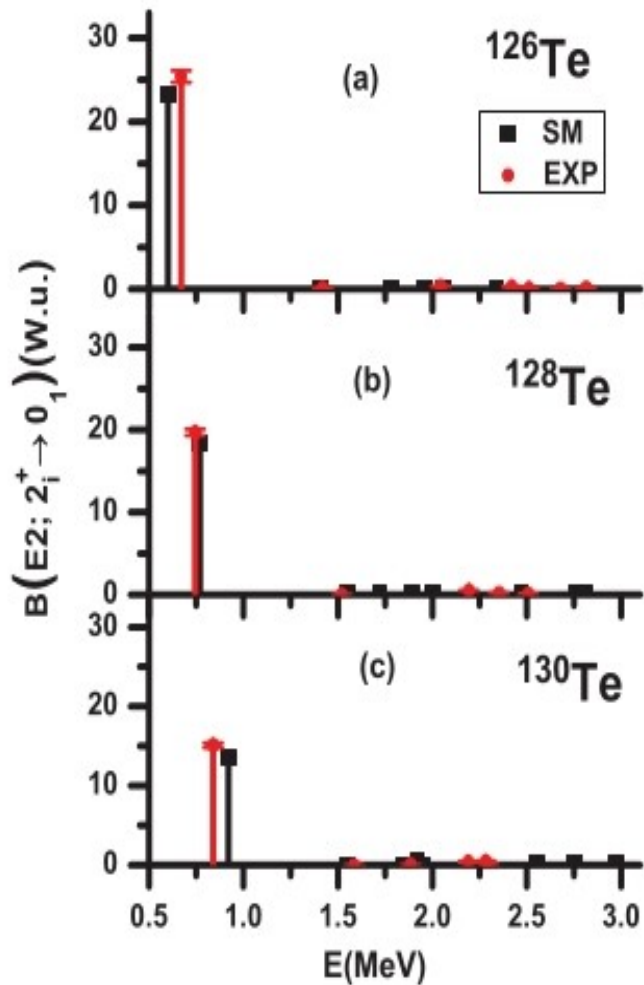
In order to infer the F-spin nature (in the Q-phonon scheme) of the states, we have calculated the ratio:

$$R_{IV/IS}(E2) = \frac{|\mathcal{M}_{(if)}^{(-)}(E2)|}{|\mathcal{M}_{if}^{(+)}(E2)|}$$

with:

$$\mathcal{M}_{(if)}^{(\pm)}(E2) = \langle 2_f^+ | [\mathcal{M}_p(E2) \pm \mathcal{M}_n(E2)] | J_i^+ \rangle$$

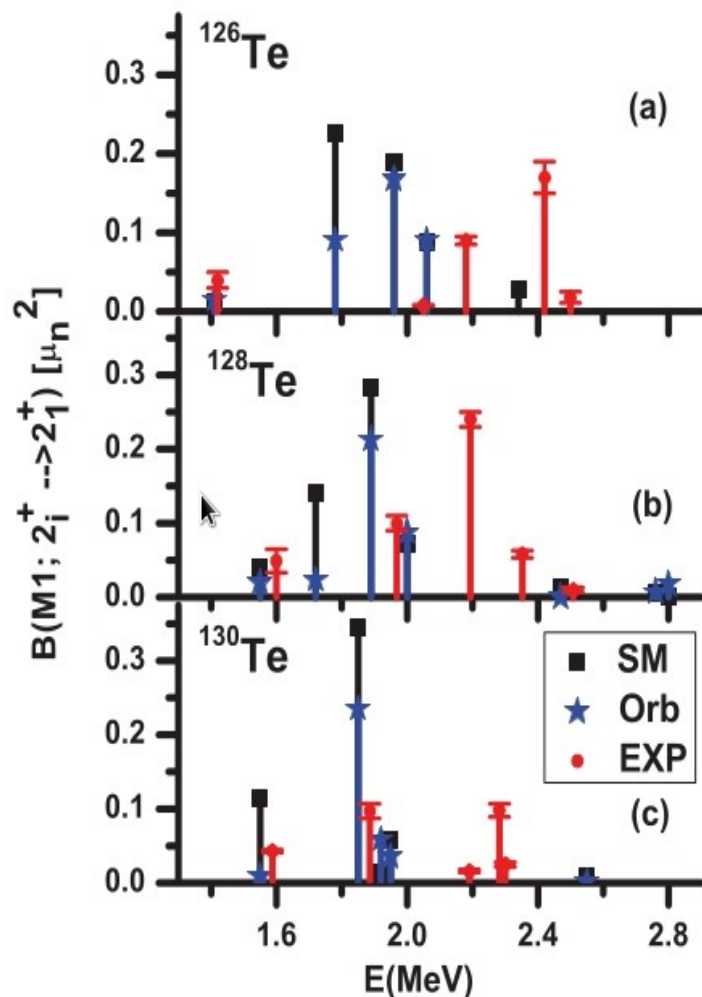
Tellurium isotopes - 2



^AX	$J_i \rightarrow J_f$	$B(E2)$		$R_{IV/IS}$
		Exp	SM	
^{126}Te	$2_1^+ \rightarrow 0_1^+$	35.4_{-7}^{+7}	23.3	0.026
	$2_2^+ \rightarrow 0_1^+$	0.15_{-2}^{+2}	0.11	17.23
	$2_3^+ \rightarrow 0_1^+$	0.36_{-2}^{+2}	0.0	
	$2_4^+ \rightarrow 0_1^+$		0.042	0.236
	$2_5^+ \rightarrow 0_1^+$	0.29_{-1}^{+2}	0.121	4.20
^{128}Te	$2_1^+ \rightarrow 0_1^+$	19.7_{-4}^{+4}	18.4	0.35
	$2_2^+ \rightarrow 0_1^+$	0.034_{-12}^{+13}	0.008	2.85
	$2_3^+ \rightarrow 0_1^+$		0.013	1.74
	$2_4^+ \rightarrow 0_1^+$	0.51_{-3}^{+2}	0.031	3.02
	$2_5^+ \rightarrow 0_1^+$	0.20_{-2}^{+2}	0.175	16.52
	$2_6^+ \rightarrow 0_1^+$	0.011_{-2}^{+2}	0.069	0.00
^{130}Te	$2_1^+ \rightarrow 0_1^+$	15.1_{-3}^{+3}	13.55	0.23
	$2_2^+ \rightarrow 0_1^+$	$< 0.013_{-1}^{+1}$	0.02	3.37
	$2_3^+ \rightarrow 0_1^+$	0.028_{-4}^{+4}	0.002	2.43
	$2_4^+ \rightarrow 0_1^+$	0.39_{-4}^{+4}	0.37	14.8
	$2_5^+ \rightarrow 0_1^+$	0.47_{-4}^{+5}	0.002	3.0
	$2_6^+ \rightarrow 0_1^+$	0.018_{-4}^{+4}	0.05	1.41
^{132}Te	$2_1^+ \rightarrow 0_1^+$	10(1)	9.26	0.025
	$2_2^+ \rightarrow 0_1^+$	0.5 (1)	0.03	4.83
	$2_3^+ \rightarrow 0_1^+$		0.002	2.71
	$2_4^+ \rightarrow 0_1^+$		0.213	3.96

D. Bianco, N. Lo Iudice, F. Andreozzi, A. Porrino, F. Knapp, Phys. Rev. C 86, 044325 (2012)

Tellurium isotopes - 3

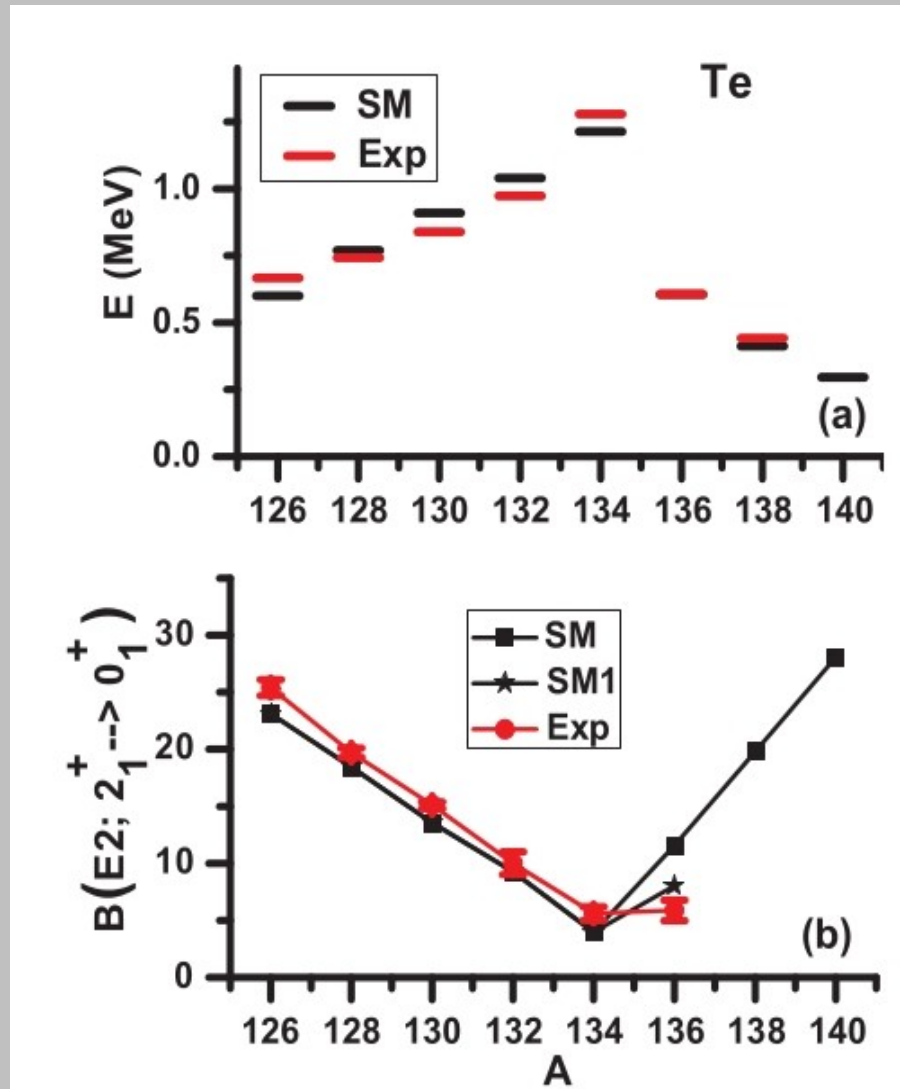


^AX	$J_i \rightarrow J_f$	$B(E2)$		$R_{IV/IS}$
		Exp	SM	
^{126}Te	$2_2^+ \rightarrow 2_1^+$	45_{-4}^{+5}	23.2	0.53
	$2_3^+ \rightarrow 2_1^+$	0.001_{-1}^{+1}	0.12	1.25
	$2_4^+ \rightarrow 2_1^+$	0.00	0.004	3.16
	$2_5^+ \rightarrow 2_1^+$	2.1_{-1}^{+1}	0.02	1.29
	$2_6^+ \rightarrow 2_1^+$	0.95_{-8}^{+7}	0.13	6.22
^{128}Te	$2_2^+ \rightarrow 2_1^+$	27.7_{-94}^{+100}	21.04	0.44
		0.25_{-25}^{+23}		
	$2_3^+ \rightarrow 2_1^+$	23.9_{-23}^{+24}	3.77	0.58
		0.42_{-6}^{+5}		
	$2_4^+ \rightarrow 2_1^+$	0.038_{-8}^{+15}	0.20	0.71
		36.4_{-26}^{+21}		
^{130}Te	$2_5^+ \rightarrow 2_1^+$	0.30_{-3}^{+3}	0.00	2.5
		8.3_{-8}^{+7}		
	$2_6^+ \rightarrow 2_1^+$	0.49_{-12}^{+15}	0.80	2.94
		0.11_{-2}^{+2}		
	$2_2^+ \rightarrow 2_1^+$	$< 21_{-1}^{+1}$	3.40	0.27
		$< 0.073_{-2}^{+2}$		
^{132}Te	$2_3^+ \rightarrow 2_1^+$	34_{-3}^{+3}	0.003	0.82
		2.2_{-2}^{+3}		
	$2_4^+ \rightarrow 2_1^+$	3.4_{-4}^{+4}	10.34	0.33
		0.27_{-3}^{+4}		
	$2_5^+ \rightarrow 2_1^+$	16_{-2}^{+2}	5.18	0.38
		0.29_{-3}^{+3}		
^{130}Te	$2_6^+ \rightarrow 2_1^+$	4.5_{-5}^{+5}	0.34	2.30
		0.36_{-4}^{+4}		
	$2_2^+ \rightarrow 2_1^+$	0-20	1.522	0.21
	$2_3^+ \rightarrow 2_1^+$		0.494	0.62
		0.149	0.126	
		6.134	0.10	

Tellurium isotopes - 4

$J_i^\pi \rightarrow J_f^\pi$	^{134}Te	^{136}Te	^{138}Te	^{140}Te
	$B(E2)$ (W.u.)			
$2_1 \rightarrow 0_1$	3.94	11.54	19.82	28.06
$2_2 \rightarrow 0_1$	0.75	0.058	0.21	0.33
$2_3 \rightarrow 0_1$	0.83	0.52	0.05	0.08
$2_4 \rightarrow 0_1$	1.11	0.52	0.17	0.07
$2_5 \rightarrow 0_1$	0.05	0.01	0.05	0.01
$2_6 \rightarrow 0_1$	0.11	0.03	0.09	0.15
$2_2 \rightarrow 2_1$	0.32	7.15	1.12	1.63
$2_3 \rightarrow 2_1$	0.39	0.02	1.42	1.52
$2_4 \rightarrow 2_1$	4.69	0.07	0.67	0.13
$2_5 \rightarrow 2_1$	0.02	0.09	0.03	0.01
$2_6 \rightarrow 2_1$	0.02	0.07	0.05	0.19
	$B(M1)$ (μ_N^2)			
$2_2 \rightarrow 2_1$	0.00	0.04	0.00	0.00
$2_3 \rightarrow 2_1$	0.00	0.24	0.00	0.00
$2_4 \rightarrow 2_1$	0.00	0.19	0.02	0.01
$2_5 \rightarrow 2_1$	0.00	0.02	0.02	0.00
$2_6 \rightarrow 2_1$	0.00	0.17	0.00	0.06

Tellurium isotopes - 5



${}^A X$	$J_i \rightarrow J_f$	$B(E2)$		$R_{v/\pi}(E2)$
		EXP	SM	SM
${}^{134}\text{Sn}$	$2_1^+ \rightarrow 0_1^+$	1.42(25)	1.71	
	$4_1^+ \rightarrow 2_1^+$		1.71	
	$6_1^+ \rightarrow 4_1^+$	0.89 (17)	0.86	
${}^{134}\text{Te}$	$2_1^+ \rightarrow 0_1^+$	5.60(64)	3.94	
	$4_1^+ \rightarrow 2_1^+$	4.3	4.55	
	$6_1^+ \rightarrow 4_1^+$	2.04	2.05	
${}^{136}\text{Te}$	$2_1^+ \rightarrow 0_1^+$	5.87(87)	11.54	2.6
	$4_1^+ \rightarrow 2_1^+$		16.44	
	$6_1^+ \rightarrow 4_1^+$		14.75	
	$8_1^+ \rightarrow 6_1^+$		12.88	
	$10_1^+ \rightarrow 8_1^+$		12.46	
${}^{138}\text{Te}$	$2_1^+ \rightarrow 0_1^+$		19.82	4.4
	$4_1^+ \rightarrow 2_1^+$		28.73	
	$6_1^+ \rightarrow 4_1^+$		29.66	
	$8_1^+ \rightarrow 6_1^+$		22.92	
${}^{140}\text{Te}$	$10_1^+ \rightarrow 8_1^+$		25.17	
	$2_1^+ \rightarrow 0_1^+$		28.06	7.4

D. Bianco, N. Lo Iudice, F. Andreozzi, A. Porrino, F. Knapp, Phys. Rev. C 88, 024303 (2013)

Conclusions

- It is extremely important to verify the reliability of our SM predictions by new independent theoretical investigations.
- It is even more crucial to test them by new extensive and conclusive experiments, especially since the original value of the $B(E2; 2^+ \rightarrow 0^+)$ in ^{136}Te has undergone several revisions.
- This need of new experimental data is even more urgent for Xenon isotopes, since the transition measurement currently available above $N=84$ are not conclusive.

Thank you

Additional Slides

Tellurium isotopes - 1

The agreement with the experiment is good, in general, even if there are not all the spin-orbit partners for the M1

